Available online at www.sciencedirect.com
ScienceDirect
International Journal of Heat and Mass Transfer 50 (2007) 3718–3727
International Journal of HEAT and MASS TRANSFER
www.elsevier.com/locate/ijhmt

Impingement heat transfer of staggered arrays of air jets confined in a channel

Jung-Yang San *, Yi-Ming Tsou, Zheng-Chieh Chen

Department of Mechanical Engineering, National Chung Hsing University, 250 Kuo-Kuang Road, Taichung, Taiwan, ROC

Received 11 March 2006; received in revised form 24 February 2007
Available online 27 April 2007

Abstract

Impingement heat transfer of circular air jets confined in a channel was experimentally investigated. The impingement plate was exerted with a constant surface heat flux. Five jets, including one center jet and four neighboring jets, in staggered arrays were considered. The considered jet Reynolds number (Re) was in the range 5000–15,000; the jet height-to-jet diameter ratio (H/d) was in the range 1.0–4.0; the jet spacing-to-jet diameter ratio (S/d) was in the range 4.0–8.0; the jet plate width-to-jet diameter ratio (W/d) was in the range 6.25–18.75. Two jet plate length-to-jet diameter ratio (L/d), 31.7 and 83.3, were individually arranged. For the center jet with a specific Reynolds number, its stagnation Nusselt number was found to linearly increase with the jet Reynolds number of the four neighboring jets. For all the five jets with the same Reynolds number, the correlation result shows that the stagnation Nusselt number of the center jet is proportional to the 0.7 power of the Re and the -0.49 power of the W/d. A weak dependence of the stagnation Nusselt number on H/d, S/d and L/d was found.
© 2007 Elsevier Ltd. All rights reserved.

Keywords: Jet; Stagnation Nusselt number; Impingement heat transfer

1. Introduction

Jet impingement is quite effective to achieve a high heat/mass transfer rate on the surface of an object. In the steel or glass industry, impinging jets are applied to temper products after rolling. In the aviation industry, impinging jets are used for cooling turbine vanes in gas turbine engines. In the electronics industry, impinging jets are applied to cool electronic components in order to meet the demand of compactness and high power consumption. In additional to the above applications in cooling, in the paper industry impinging jets are adopted to enhance drying processes.

A large amount of work relating to single-jet impingement heat transfer was elaborated by Garimella and Rice [1], Fitzgerald and Garimella [2] and San et al. [3]. Recently, Guerra et al. [4] performed an experiment to measure the flow velocity and temperature for a confined impinging jet. Yang and Wang [5] used the k–ε turbulence model to show a pair of rotating vortices in a channel for a flow with an inclined impinging jet. San and Shiao [6] successfully expressed the stagnation Nusselt number for a confined impinging jet as a function of jet Reynolds number, jet height-to-jet diameter ratio, jet plate length-to-jet diameter ratio and jet plate width-to-jet diameter ratio.

Similarly, a considerable amount of research relating to multiple-jet impingement heat transfer was also conducted in the past few decades. Gardon and Akfirat [7] investigated the heat transfer characteristics of two-dimensional air jets impinging perpendicular to an isothermal flat plate. Kercher and Tabakoff [8] measured the average Nusselt number of an in-line array of confined circular air jets impinging perpendicular to a flat plate. Metzger et al. [9],

* Corresponding author. Tel.: +886 11 4 2220 5585; fax: +886 11 4 2285 1941.
E-mail address: jysan@dragon.nchu.edu.tw (J.-Y. San).

0017-9310/$ - see front matter © 2007 Elsevier Ltd. All rights reserved.
doi:10.1016/j.ijheatmasstransfer.2007.02.027

Nomenclature

d	jet diameter (m)	W	jet plate width (m)
h	convctive heat transfer coefficient (W/m^2 K)	x	x-coordinate (m)
H	jet plate-to-impingement plate spacing (m)	y	y-coordinate (m)
k	thermal conductivity of air (W/m K)		
L	jet plate length (m)	*Greek symbol*	
Nu	local Nusselt number, hd/k	v	kinematic viscosity (m^2/s)
q	surface heat flux (W/m^2)		
Re	jet Reynolds number, Ud/v	*Subscripts*	
S	jet-to-jet spacing (m)	c	center jet
T_{aw}	adiabatic wall temperature (°C)	n	neighboring jet
T_w	local wall temperature (°C)	sg	stagnation point
U	jet mean velocity (m/s)		

Florschuetz et al. [10–12], Florschuetz and Isoda [13] and Florschuetz and Su [14] investigated the heat transfer characteristics of in-line and staggered arrays of circular air jets impinging on an isothermal plate.

Saripalli [15] conducted a flow visualization for multi-jet impingement. A fountain between two adjacent jets was observed. Behbahani and Goldstein [16] obtained the local Nusselt number for staggered arrays of circular air jets impinging on a constant heat flux surface. A relative maximum of Nusselt number, between two adjacent jets in the streamwise direction, was clearly observed. Slayzak et al. [17] investigated the effect of jet interaction on the local heat transfer characteristics for two-dimensional impinging jets. A maximum convective heat transfer coefficient between two stagnation lines was found. Salamah and Kaminski [18] numerically investigated the heat transfer from an array of turbulent slot jets impinging on a flat plate. A local maximum Nusselt number between two adjacent jets was also found. In addition, their modeling approach successfully captures both the stagnation region behavior and the transition to turbulence in the wall jet region. El-Gabry and Kaminski [19] used both the standard k–ε turbulence model and the low Reynolds number Yang-Shih turbulence model to simulate the heat transfer characteristics on a smooth surface under an array of angled impinging jets. The result shows that the numerical models were able to predict the periodic variation of the spanwise average Nusselt number on the impingement plate.

Huber and Viskanta [20] investigated the effect of jet-to-jet spacing on the heat transfer for confined jet arrays. The result reveals that, for large jet height (plate spacing), jet interference causes a significant degradation of the heat transfer. San and Lai [21] also investigated the effect of jet interference on the heat transfer for staggered arrays of impinging air jets. An optimum jet spacing of heat transfer was found. Dano et al. [22] investigated the effect of nozzle geometry on the heat transfer for an in-lined array of impinging jets. The heat transfer performance of the cusped ellipse nozzle appears to be superior to that of the circular nozzle.

Glodstein and Timmers [23] adopted a liquid crystal technique to visualize the isotherms on a heated plate with a multi-jet impingement. Yan et al. [24] used a 1-D transient liquid crystal scheme to investigate the impingement heat transfer on rib-roughened surfaces. The rib angle to achieve the best heat transfer performance was found to be 45°. Wang et al. [25] used a 3-D transient liquid crystal scheme to investigate the heat transfer characteristics for an in-lined impinging jet array. The result shows that increasing the cross-flow velocity would deteriorate the heat transfer performance, but a uniform distribution of the convective heat transfer coefficient can thus be obtained.

In this work, five circular air jets, including one center jet and four neighboring jets, confined in a channel were considered (Fig. 1). The five jets were arranged in various staggered arrays. It intended to apply these jet arrays for cooling electronic devices. Although the results in the literature provide many insights into the physical phenomena of jet impingement. Yet, their jet arrays and flow arrangements are quite different from the present considered cases. In addition, very few of them were centered on establishing heat transfer correlations for multi-jet impingement. This results in both uncertainty and inconvenience for using these available data in designing a multi-jet impingement cooling system. In view of these reasons, in this work, an investigation of the heat transfer characteristics for the considered jet arrays was conducted. First, the dependence of the stagnation Nusselt number of the center jet on four neighboring jets was investigated. Second, for all the five jets with the same Reynolds number, the effects of jet-to-jet spacing (S), jet Reynolds number (Re), jet height (H), jet plate width (W) and jet plate length (L) on the stagnation Nusselt number of the center jet were individually determined. Third, through the measured data, it expected to obtain a simple correlation for the stagnation Nusselt number of the center jet.

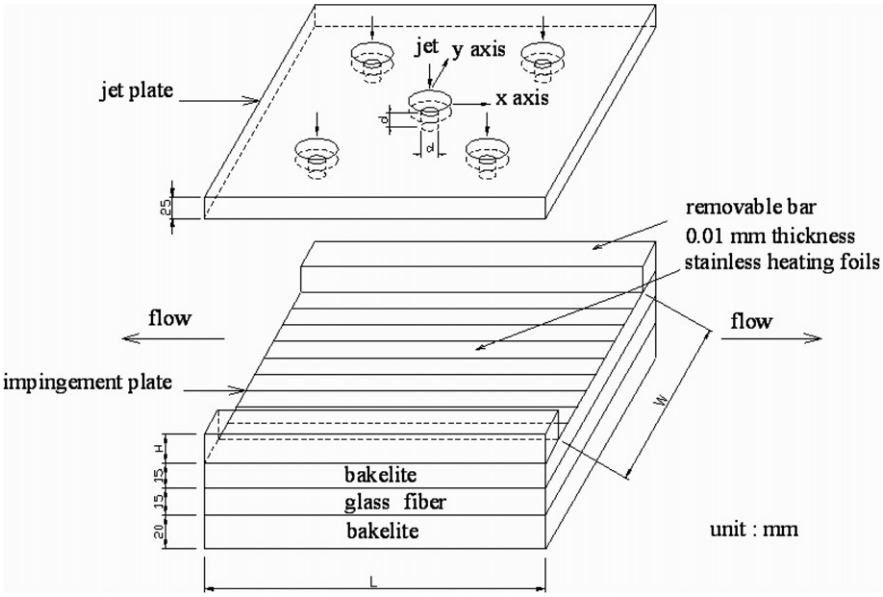

Fig. 1. Impingement plate and jet plate.

2. Experimental apparatus and error analysis

In this work, the experimental apparatus and procedure are much the same as those in previous work [3,6,21]. Fig. 2 shows the experimental setup for the measurement. The high pressure air was supplied by a reciprocating air compressor. In the experiment, the air pressure in the compressor tank was maintained in the range 700–800 kPa. The high pressure air was dehydrated by arranging it to pass through two vapor compression type dehumidifiers. Following, the air was purified using three adsorption columns filled with granular activated carbon. Then the air was stored in a large surge tank in which the pressure was maintained at 405 kpa. The volumetric flowrates of the air passing through the five jet holes on the jet plate were metered using five calibrated rotameters, respectively. The diameter of the jet holes is 6 mm. In the experiment, by varying the volumetric flowrate of the air, a specific jet Reynolds numbers (Re) can be arranged.

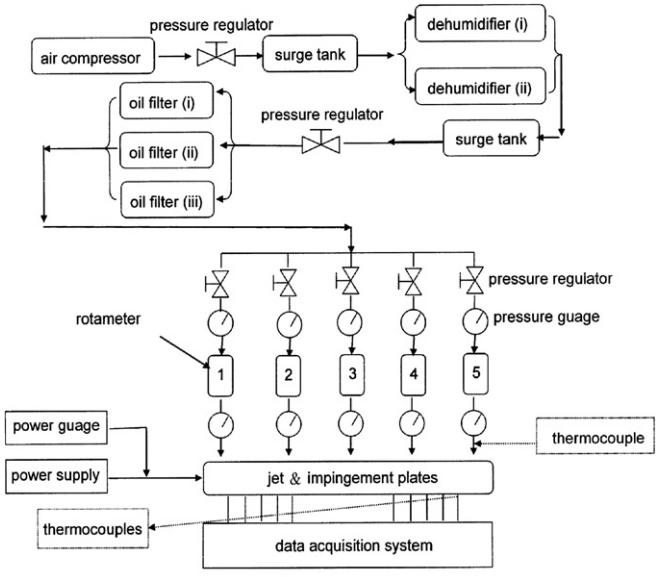

Fig. 2. Experimental apparatus.

The jet plate was designed to be easily replaced from the top of the experimental setup (Fig. 1). In this work, totally four jet plates with different jet-to-jet spacings and lengths were used. For three of them, the length (L) is 500 mm and the jet spacings (S) are 24, 36 and 48 mm, respectively. The other one is with length of 190 mm and jet spacing of 36 mm. The jet height can also be easily adjusted by leveling up the support of the jet plate. In the experiment, three different jet heights (6, 12 and 24 mm) were individually considered.

Nine 0.01 mm-thickness stainless steel heating foils were stuck on the impingement plate. The width of each heating foil is 12.5 mm and the length is 400 mm. An electric current, supplied by an Agilent E3610A DC power supply unit, was arranged to flow through the heating foils to generate a uniform surface heat flux. The detailed wiring of the heating foils can be found in an earlier published paper [6]. In measurement of the stagnation Nusselt number of the center jet, two removable rectangular bars were carefully placed on the two outer edges of the heated foils (along the x-axis) to form a channel between the jet plate and impingement plate. In doing so, the width of the channel (effective jet plate width) becomes the same as that of the heated foils. Seventy-six thermocouples were orderly embedded below the middle heating foil. The spacing between any two adjacent thermocouples is 3 mm.

The jet plate was designed to be able to move in the x and y directions (Fig. 1) individually by adjusting two screws. Two linear photo-electronic scales with a smallest

readout of 0.001 mm were used to position the jet plate. The measured temperatures were recorded by a HP-34970A data acquisition unit.

An uncertainty analysis was performed for the experiment. In the flowrate measurement, the inaccuracy of the rotameters causes a maximum 5% error on the jet Reynolds number. In the heat transfer measurement, both the inaccuracy due to the temperature measurement and the inaccuracy of the surface heat flux would result in the uncertainty of the local Nusselt number. For the measurement of the stagnation Nusselt number of the center jet, the same thermocouple was used to measure the adiabatic and heated-wall temperatures. Thus the inaccuracy of the temperature measurement can be neglected. The inaccuracy of the surface heat flux was mainly attributed to radiation loss from heating foils (3.1%), non-uniformity of heating foils (4.4%), lateral solid heat conduction (2.0%) and heat loss through the insulation (0.9%). The overall uncertainty of the measured stagnation Nusselt number was evaluated to be 5.8%.

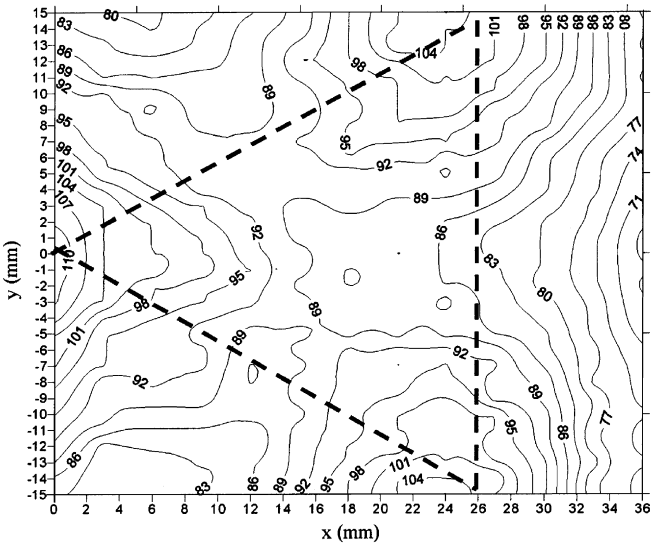

Fig. 3. Local Nusselt number distribution ($Re = 20{,}000$, $H/d = 2.0$, $W/d = 43.3$, $S/d = 5.0$ and $L/d = 83.3$).

3. Local Nusselt number

The local Nusselt number (Nu) on the impingement plate is a function of several variables. As indicated in previous work [6,21], this local Nusselt number is relevant to heated-surface geometry, surface heat flux, jet diameter, jet-to-jet spacing, plate spacing, jet plate size, location on impingement plate, jet velocity, exit flow direction and orifice aspect ratio etc. Among these variables, the surface heat flux had been verified to be almost irrelevant to the local Nusselt number [3]. Thus in the analysis this variable was excluded and a fixed value equal to 1000 W/m^2 was employed. In addition, in this work, the aspect ratio of jet orifice was selected as 1.0; the jet flow after impingement was restricted to leave through two opposite sides (x-direction) between the jet plate and impingement plate; the jet plate width was arranged to be the same as the heating foil width. With these specifications, the remaining variables can be grouped into several non-dimensional parameters, namely, H/d, S/d, W/d, L/d, Re, x/d and y/d. Hence, the local Nusselt number can be expressed as follows:

$$Nu = hd/k = [q/(T_w - T_{aw})](d/k) = f(H/d, S/d, Re, W/d, L/d, x/d, y/d). \quad (1)$$

The above function contains seven variables. Among these variables, x/d and y/d are the two giving rise to the difficulty in correlating the heat transfer data. This can be observed from the measured local Nusselt number distribution for a jet array similar to those considered in this work (Fig. 3). The work shown in Fig. 3 corresponds to a confined jet array with $Re = 20{,}000$, $H/d = 2.0$, $W/d = 43.3$, $S/d = 5.0$ and $L/d = 83.3$. For this special case, the width of heating foils is less than that of impingement plate (or jet plate). Hence, the heating foil width-to-jet diameter ratio is different from the jet plate width-to-jet diameter ratio (W/d) and it is equal to 18.75. In Fig. 3, due to symmetry of the jet array, only the heat transfer data in the positive x domain are shown. In the diagram, the peaks of the triangle (three dashed lines) indicate the locations of the three impinging jets in the positive x direction. The peak locating at the origin ($x = y = 0$) indicates the projection of the center jet (center line of jet orifice) and the other two individually indicate the projections of the two neighboring jets. As indicated, the local Nusselt number distribution for the multi-jet impingement is quite complex. Moreover, the stagnation points of the neighboring jets are affected by the center jet, as a result, they tend to move toward the center jet. In the literature, there are two ways to characterize the heat transfer performance for a jet array. One is to define an average Nusselt number, which is the mean value of the local Nusselt number over the entire surface of the impingement plate; the other is to directly use the local Nusselt number at the stagnation point. In practical applications, the former is useful to evaluate the overall heat transfer on a surface and the latter is important to predict the heat transfer at a certain spot on a surface. In this work, only the measured heat transfer data at the stagnation point of the center jet ($x = y = 0$) were investigated. In the measurement, the Re value was in the range 5000–15,000; the H/d value was in the range 1–4; the S/d value was in the range 4.0–8.0; the W/d value was in the range 6.25–18.75; two L/d values, 31.7 and 83.3, were individually considered.

4. Measured heat transfer data

In this work, five confined impinging air jets were considered. For the center jet with a specific Reynolds number (Re_c), by varying the Reynolds number of the four neighboring jets (Re_n), the effect of neighboring jets on the

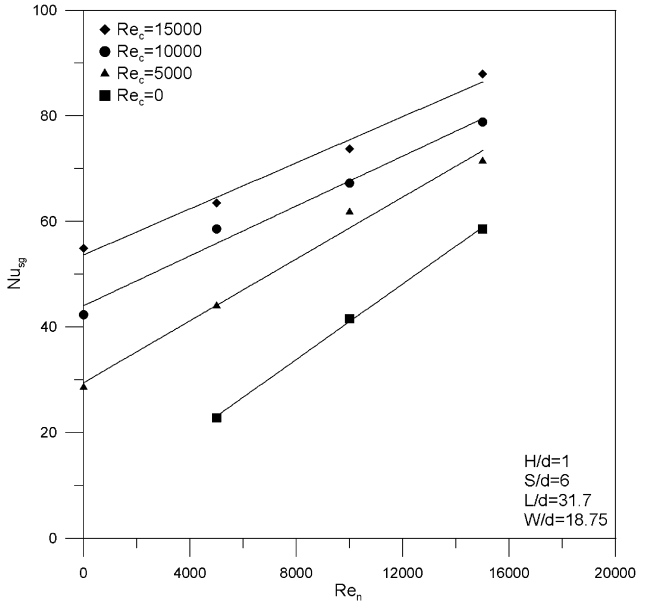

Fig. 4. Effect of Re_n on Nu_{sg}.

stagnation Nusselt number of the center jet (Nu_{sg}) was investigated. The measured result is shown in Fig. 4. As indicated, the stagnation Nusselt number of the center jet almost linearly increases with the Reynolds number of the neighboring jets. For a confined single-jet impingement, flow recirculation and mixing between the downstream heated air and the jet emanating from the jet hole would result in a degradation of the heat transfer at the stagnation point [2,6]. For the present considered multi-jet impingement, the neighboring jets block the passage for the downstream recirculation air flowing toward the center jet. The center jet is allowed to mainly mix with the flow confined within the four neighboring jets. The higher the Reynolds number of the neighboring jets, the lower the temperature of the flow confined within the four neighboring jets. Thus for the center jet with a fixed Reynolds number, the stagnation Nusselt number increases with the Reynolds number of the neighboring jets.

There are four lines shown in Fig. 4. Each line corresponds to a case with a specific Reynolds number for the center jet. As indicated, the slopes of these lines are different and they tends to decrease with an increase of the Reynolds number of the center jet. This implies that, as the Reynolds number of the center jet increases, the effect of Reynolds number of the neighboring jets on the stagnation Nusselt number of the center jet tends to decrease.

In Fig. 4, the three cases with the Re_n value of zero individually stand for three single-jet impingements with different jet Reynolds numbers. In this work, the corresponding Nu_{sg} values for the single-jet impingements were compared to the values predicted using a correlation equation, which was established in a previous work [6]. The comparison reveals a good agreement between the present data and the earlier obtained result. In Fig. 4, it is quite interesting to extrapolate the line corresponding to $Re_c = 0$ to intercept with the ordinate. As can be easily found, the corresponding Nu_{sg} value is not equal to zero. This implies that, even without impinging jets, there is still free convection between the jet plate and impingement plate.

Table 1
Category of experiments

Experiment no.	*Re*	*H*/*d*	*S*/*d*	*W*/*d*	*L*/*d*
1–27	5000, 10,000, 15,000	1, 2, 4	4, 6, 8	18.75	83.3
28–36	5000, 10,000, 15,000	1, 2, 4	6	18.75	31.7
37–42	5000, 10,000, 15,000	2, 4	6	14.58	31.7
43–51	5000, 10,000, 15,000	4	4, 6, 8	10.42	83.3
52–57	5000, 10,000, 15,000	2, 4	6	10.42	31.7
58–60	5000, 10,000, 15,000	4	4	6.25	83.3

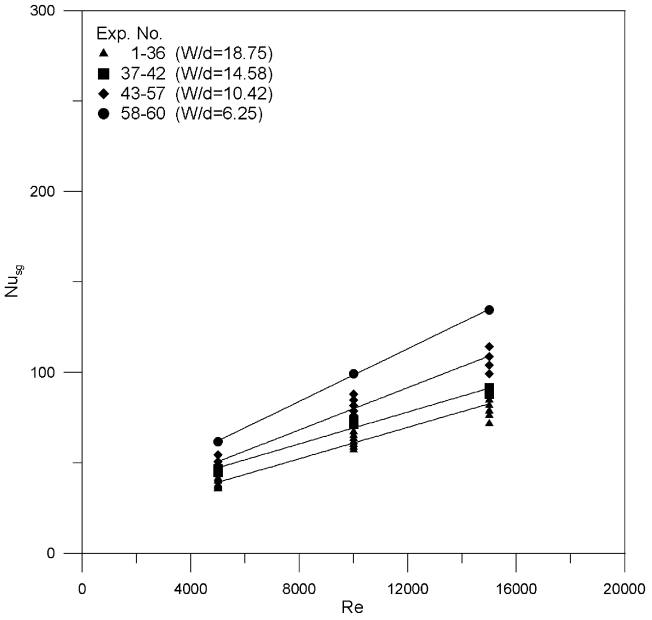

Fig. 5. Measured data of Nu_{sg}.

The main objective of this work was to determine the heat transfer characteristics at the stagnation Nusselt number of the center jet for all the five jets with the same Reynolds number ($Re_c = Re_n = Re$). For this purpose, totally 60 sets of experiment were conducted. The corresponding *Re*, *H*/*d*, *S*/*d*, *W*/*d* and *L*/*d* values for the 60 sets of experiment were summarized in Table 1. Fig. 5 shows the measured data of the stagnation Nusselt number of the center jet. As clearly indicated, the stagnation Nusselt number tends to increase with the jet Reynolds number and decrease with an increase of the *W*/*d*.

5. Correlation of stagnation Nusselt number

Existing correlations express the Nusselt number for jet impingement as a function of Re^c [7,10–13]. The exponent, *c*, falls in the range 0.45–0.8. In an earlier work [6] performed in the same laboratory as the present work, for a confined single-jet impingement, the exponent, *c*, was found to be 0.638. In this work, the same procedure was

applied to correlate the present measured data. Figs. 6–9 show the correlation results for the W/d value of 6.25, 10.42, 14.58 and 18.75, respectively. As indicated, for a set of H/d, S/d, L/d and W/d values, the three Nu_{sg} values individually corresponding to the Re values of 5000, 10,000 and 15,000 were successfully fitted into a straight line in a diagram with ln(Re) as the abscissa and with ln(Nu) as the ordinate. Different sets of H/d, S/d, L/d and W/d values yield different straight lines. However, their slopes are quite close. In the analysis, a common slope of 0.7 was selected

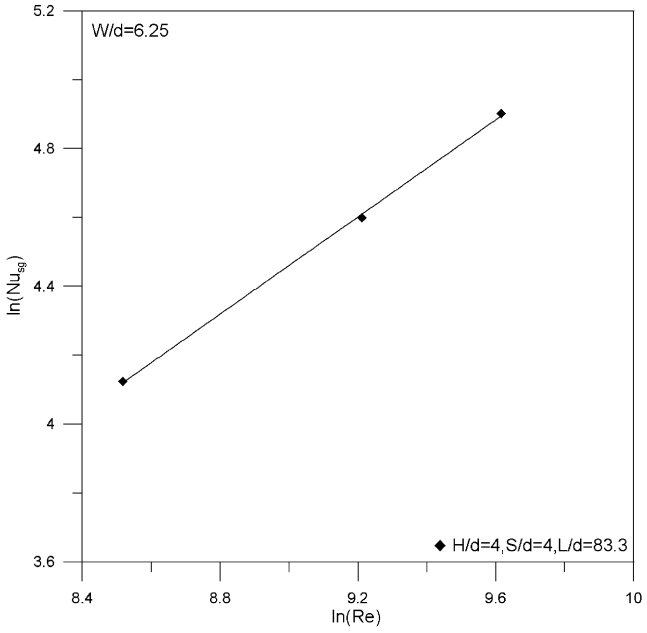

Fig. 6. Relationship between Nu_{sg} and Re for $W/d = 6.25$.

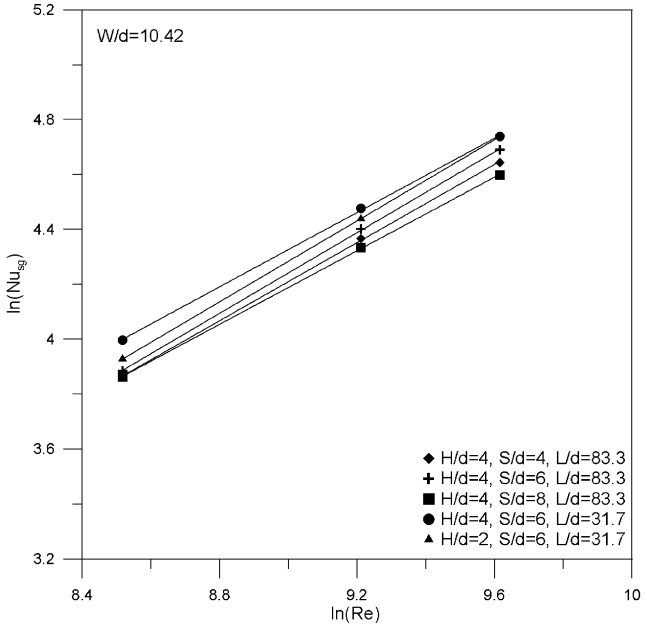

Fig. 7. Relationship between Nu_{sg} and Re for $W/d = 10.42$.

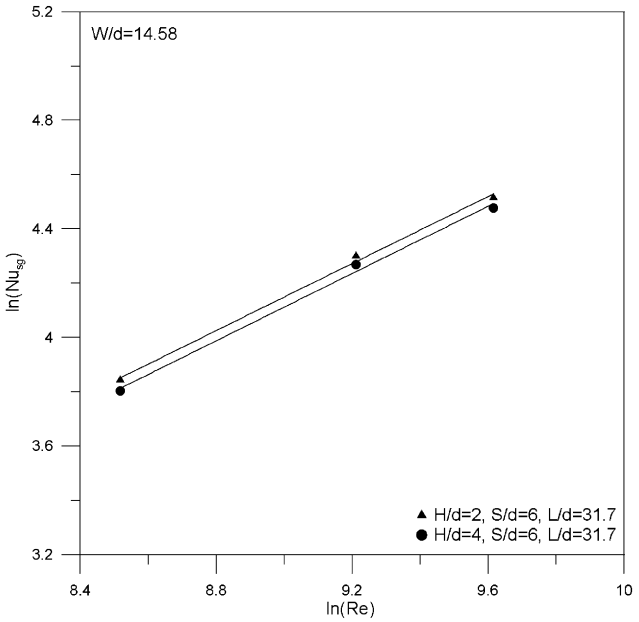

Fig. 8. Relationship between Nu_{sg} and Re for $W/d = 14.58$.

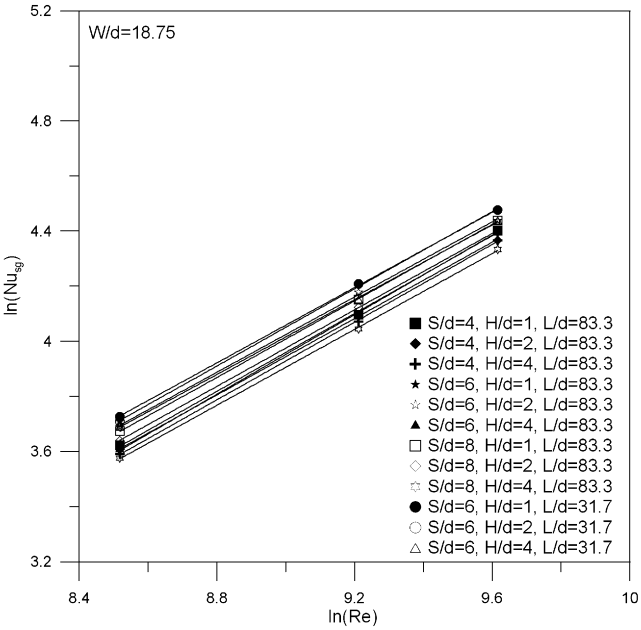

Fig. 9. Relationship between Nu_{sg} and Re for $W/d = 18.75$.

for all these straight lines. This means that the exponent, c, was selected as 0.7.

In Fig. 10, the abscissa is ln(W/d) and the ordinate is ln($Nu_{sg}/Re^{0.7}$). After plotting the measured data into the diagram, those data with the same H/d, S/d and L/d values were also fitted with a straight line. As indicated, the slopes of all these straight lines are close to -0.49. This means that the relationship, $Nu_{sg} \propto (W/d)^{-0.49}$, exists. Fig. 10 also shows that, for the cases with the same ln(W/d) value, the deviation among the corresponding ln($Nu_{sg}/Re^{0.7}$) values is not large. This implies that the dependence of the

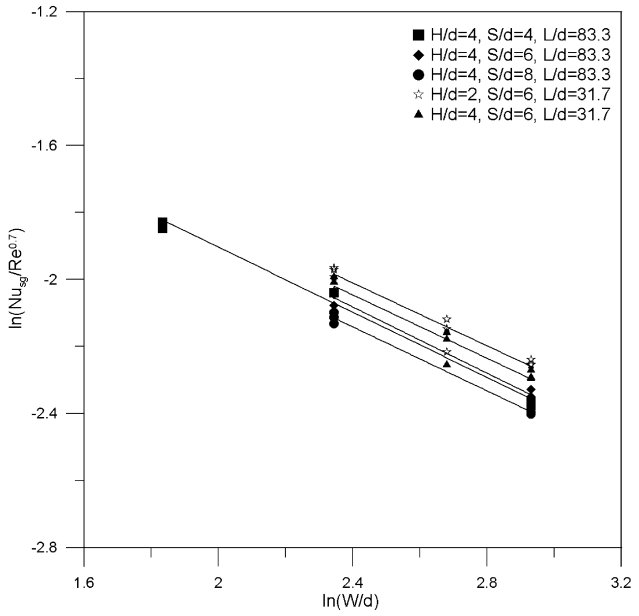

Fig. 10. Relationship between Nu_{sg} and W/d.

stagnation Nusselt number on H/d, S/d and L/d is small. Based on the current measured data, the following is a detailed analysis of the effects of H/d, S/d and L/d on the stagnation Nusselt number.

Fig. 11 indicates that the Nu_{sg} slightly decreases with an increase of the H/d. For a confined single-jet impinging on a flat plate [6], the stagnation Nusselt number was found to be proportional to the -0.3 power of the H/d. This phenomenon was attributed to a larger spacing between the jet plate and impingement plate allowing a longer distance for the jet to mix with the downstream recirculation flow. Hence, the stagnation Nusselt number decreases with an increase of the H/d. For a jet impinging on a flat plate, the pattern of its recirculation flow is in the form of a toroid [2]. In other words, the recirculation flow would flow from all the directions toward the jet and then mix with it. For the present considered multi-jet impingement, a recirculation flow is also expected to flow from all the directions toward the jet arrays and then mixes with the jet arrays. However, to the center jets of the jet arrays, this recirculation flow is largely blocked by the four neighboring jets. This might lessen the influence of recirculation flow on the stagnation Nusselt number. Consequently, the dependence of the stagnation Nusselt number on H/d becomes small.

Fig. 12 shows that the effect of S/d on the stagnation Nusselt number is also weak. In a previous work [21], for confined jet arrays an optimum S/d was found. This optimum S/d corresponds to a maximum Nu_{sg} for the center jet. In that work, similar to the one considered in Fig. 3, the heating foil width-to-jet diameter ratio is less than the jet plate width-to-jet diameter ratio (W/d). The former is equal to 37.5 and the latter is 86.6. The existence of the maximum Nu_{sg} was mainly attributed to two reasons. One of the reasons is the occurrence of a jet interference within the jet arrays for small S/d. This jet interference weakens the strength of the center jet and it also enhances the flow mixing between the jet array and recirculation flow. The smaller the S/d, the stronger the jet interference. Hence, for small S/d, the Nu_{sg} tends to decrease with the S/d. The other reason to cause the maximum Nu_{sg} results from an increase of the heat transfer area within the jet array for an increase of the S/d. This increase in the heat transfer area would deteriorate the heat transfer at the stagnation point. Moreover, for an increase of the S/d, more recirculation flow might penetrate through the spac-

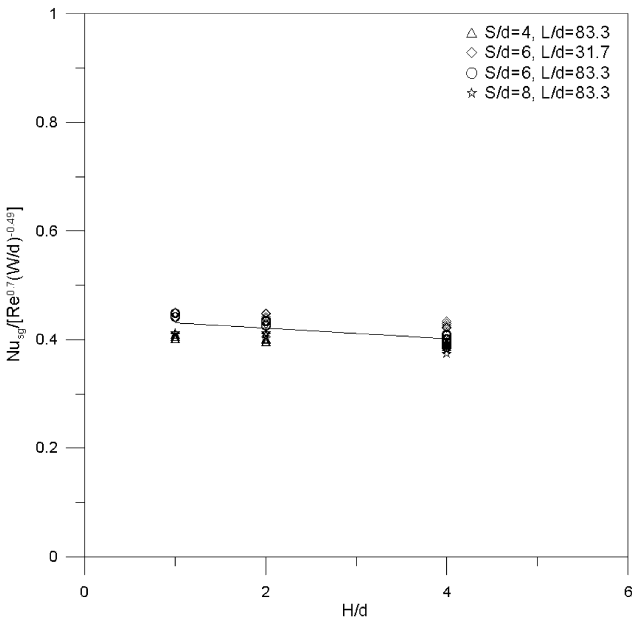

Fig. 11. Effect of H/d on Nu_{sg}.

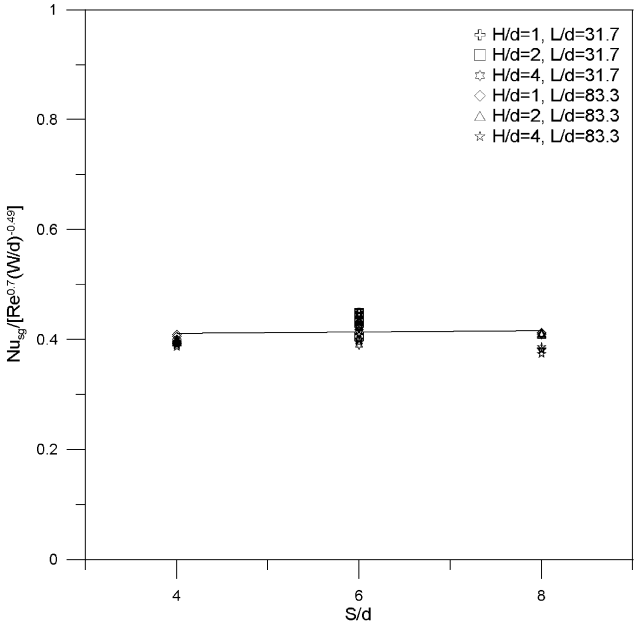

Fig. 12. Effect of S/d on Nu_{sg}.

ings between the neighboring jets. Before encountering the center jet, this recirculation flow might also experience a weaker flow mixing with the neighboring jets. This could result in a higher recirculation flow temperature and consequently deteriorate the heat transfer at the stagnation point. Hence, for large S/d, the Nu_{sg} tends to decrease with an increase of the S/d.

In the present work, the y-direction flow was blocked by the two removable bars individually locating on the two outer edges of the heated foils. Hence, the traveling distance for the y-direction recirculation flow is equal to a half of the heating foil width ($=W/2$). As long as the W/d remains the same, this traveling distance would not change. Moreover, in this work the considered heating foil width-to-jet diameter ratios ($=W/d$) are in the range 6.25–18.75 which are much smaller than that considered in the previous work. A strong flow mixing is expected not only within the jet arrays, but also between the jet arrays and side walls (removable bars). Hence, the effect of S/d on the temperature of the y-direction recirculation flow could be small. This might result in a weak dependence of the stagnation Nusselt number on S/d. The significance of the y-direction recirculation flow in affecting the stagnation Nusselt number will be explained later in this paper.

In Fig. 13, the abscissa is L/d and the ordinate is $\ln\{Nu_{sg}/[Re^{0.7}(W/d)^{-0.49}]\}$. After plotting all the 60 sets of experimental data into the diagram, the result shows that the Nu_{sg} tends to slightly decrease with an increase of the L/d. For a confined single-jet impingement [6], the stagnation Nusselt number was also found to be a function of L/d. The larger the L/d, the smaller the stagnation Nusselt number. This phenomenon was attributed to an increase of the strength of the flow recirculation between the jet and downstream heated flow for an increase of the L/d. However, for the present considered multi-jet impingement, the x-direction recirculation flow could be largely blocked by the neighboring jets. Thus, the effect of L/d on the stagnation Nusselt number is much weaker than that for a confined single-jet impingement [6].

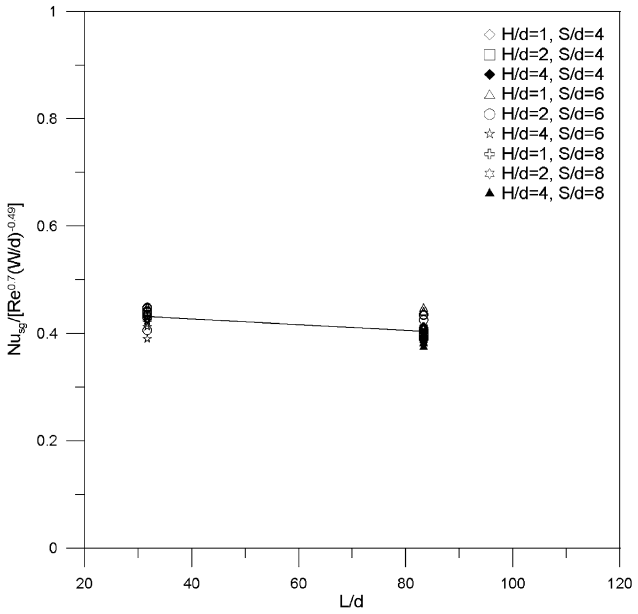

Fig. 13. Effect of L/d on Nu_{sg}.

Comparing Fig. 13 with Fig. 10, it clearly indicates that the stagnation Nusselt number of the center jet considerably decreases with an increase of the W/d, but it appears to have a weak dependence on the L/d. As indicated in Fig. 1, for the considered jet arrays, the spacing between the two neighboring jets aligned perpendicular to the flow direction of the spent air (S) is smaller than that parallel to the flow direction of the spent air ($\sqrt{3}S$). Hence, the y-direction recirculation flow should be easier to penetrate through the spacing between the neighboring jets than the x-direction recirculation flow does. Moreover, in this work, the spent air was restricted to flow only in two opposite directions (x-direction) and the y-direction flow was completely blocked by the side walls. Hence, the y-direction recirculation flow should be much stronger than the x-direction recirculation flow. This two reasons might cause the flow mixing between the center jet and y-direction recirculation flow to be much stronger than that between the center jet and x-direction recirculation flow. For an increase of the W/d, the heat transfer area covered by the y-direction recirculation flow would increase. This results in a temperature rise of the y-direction recirculation flow. Following, through the strong flow mixing between the center jet and y-direction recirculation flow, the stagnation Nusselt number is thus considerably affected. For an increase of the L/d, the strength of the x-direction recirculation flow would also increase. As explained in the above, this x-direction recirculation flow might be largely blocked by the neighboring jets aligned perpendicular to the direction of the spent air. Hence, the effect of W/d on the stagnation Nusselt number appears to be much stronger than that of L/d.

Based on the above analysis, a correlation for the stagnation Nusselt number of the center jet was established. In the correlation, the effects of H/d, S/d and L/d on the stagnation Nusselt number were neglected. This correlation can be expressed as follows:

$$Nu_{sg} = 0.41 Re^{0.7}(W/d)^{-0.49}$$
$$\text{For} \quad \begin{matrix} 5000 \leqslant Re \leqslant 15{,}000, & 1 \leqslant H/d \leqslant 4 \\ 6.25 \leqslant W/d \leqslant 18.75, & 31.7 \leqslant L/d \leqslant 83.3. \end{matrix} \tag{2}$$

Eq. (2) can be used to predict the stagnation Nusselt number of the center jet for the considered jet arrays in the indicated range of operating conditions. However, it has to mention here, due to limitation of the current experimental apparatus, only three sets of data with different jet Reynolds numbers were measured for the W/d value of 6.25. Hence, a stricter range of W/d for the above correlation should be $10.42 \leqslant W/d \leqslant 18.75$. In this work, a comparison between the measured data and corresponding predicted values was performed. It shows that the mean

deviation and maximum deviation are 5.4% and 10.6%, respectively.

In this work, small jet arrays containing only five impinging jets were considered. The result shows that the effect of H/d on the stagnation Nusselt number of the center jet can be neglected. For large jet arrays, such as those applied for cooling turbine vanes in gas turbine engines, the downstream jets would encounter a strong cross flow resulting from the spent air of the upstream jets. For an increase of the H/d, this cross flow might significantly weaken the strength of the downstream jets and thus deteriorate the heat transfer. Hence, the H/d could be an important factor affecting the stagnation Nusselt number of the downstream jets. This should be noticed in using the present obtained correlation.

6. Conclusions

In this work, the effect of Reynolds number of the four neighboring jets on the stagnation Nusselt number of the center jet was investigated. The result shows that, for the center jet with a fixed Reynolds number, the stagnation Nusselt number almost linearly increases with the Reynolds number of the four neighboring jets.

For the five jets with the same Reynolds number, likewise, the stagnation Nusselt number of the center jet also increases with the Reynolds number. In the considered range of operating conditions, the experimental data reveal that the dependence of the stagnation Nusselt number on jet height-to-jet diameter ratio (H/d) and jet spacing-to-jet diameter ratio (S/d) is weak. This probably is because there is a strong flow mixing within the jet arrays and between the jet arrays and side walls. This strong flow mixing causes the effect of H/d and S/d on the stagnation Nusselt number to become insignificant.

The result also shows that the stagnation Nusselt number of the center jet considerably decreases with an increase of the jet plate width-to-jet diameter ratio (W/d), but it appears to have a weak dependence on the jet plate length-to-jet diameter ratio (L/d). For a confined single-jet impingement [6], it is known that an increase of the jet plate length would enhance the mixing between the jet and downstream recirculation flow. Consequently, it results in a decrease of the stagnation Nusselt number. To the center jets of the present considered jet arrays, the x-direction downstream recirculation flow might be largely blocked by the four neighboring jets. Thus the effect of jet plate length on the stagnation Nusselt number becomes insignificant. For the considered staggered arrays of impinging jets, the spacing between the two neighboring jets aligned perpendicular to the flow direction of the spent air (S) is smaller than that parallel to the flow direction of the spent air ($\sqrt{3}S$). Hence, the y-direction recirculation flow should be easier to penetrate through the spacing between the neighboring jets than the x-direction recirculation flow does. Moreover, in this work, the spent air was restricted to flow only in two opposite directions (x-direction) and the y-direction flow was completely blocked by the side walls. Hence, the y-direction recirculation flow is expected to be stronger than the x-direction recirculation flow. These two reasons might cause the effect of W/d on the stagnation Nusselt number to be much stronger than that of L/d.

The measured data of stagnation Nusselt number were correlated into a simple form. The result indicates that the stagnation Nusselt number is proportional to the 0.7 power of the jet Reynolds number and the -0.49 power of the jet plate width-to-jet diameter ratio (W/d). The effect of H/d, S/d and L/d on the stagnation Nusselt number appears to be insignificant.

References

[1] S.V. Garimella, R.A. Rice, Confined and submerged liquid jet impingement heat transfer, J. Heat Transfer 117 (1995) 871–877.
[2] J.A. Fitzgerald, S.V. Garimella, A study of the flow field of a confined and submerged impinging jet, Int. J. Heat Mass Transfer 41 (8–9) (1998) 1025–1034.
[3] J.Y. San, C.H. Huang, M.H. Shu, Impingement cooling of a confined circular air jet, Int. J. Heat Mass Transfer 40 (6) (1997) 1355–1364.
[4] D.R.S. Guerra, J. Su, P. Atila, A.P. Silva Freire, The near wall behavior of an impinging jet, Int. J. Heat Mass Transfer 48 (14) (2005) 2829–2840.
[5] Y.T. Yang, Y.X. Wang, Three-dimensional numerical simulation of an inclined jet with cross-flow, Int. J. Heat Mass Transfer 48 (19–20) (2005) 4019–4027.
[6] J.Y. San, W.Z. Shiao, Effects of jet plate size and plate spacing on the stagnation Nusselt number for a confined circular air jet impinging on a flat plate, Int. J. Heat Mass Transfer 49 (19–20) (2006) 3477–3486.
[7] R. Gardon, J.C. Akfirat, Heat transfer characteristics of impinging two-dimensional air jets, J. Heat Transfer 88 (1966) 101–108.
[8] D.M. Kercher, W. Tabakoff, Heat transfer by a square array of round air jets impinging perpendicular to a flat surface including the effect of spent air, J. Eng. Power 92 (1970) 73–82.
[9] D.E. Metzger, L.W. Florschuetz, D.I. Takeuchi, R.D. Behee, R.A. Berry, Heat transfer characteristics for inlined and staggered arrays of circular jets with crossflow of spent air, J. Heat Transfer 101 (1979) 526–531.
[10] L.W. Florschuetz, R.A. Berry, D.E. Metzger, Periodic streamwise variations of heat transfer coefficients for inlined and staggered arrays of circular jets with crossflow of spent air, J. Heat Transfer 102 (1980) 132–137.
[11] L.W. Florschuetz, C.R. Truman, D.E. Metzger, Streamwise flow and heat transfer distributions for jet array impingement with crossflow, J. Heat Transfer 103 (1981) 337–342.
[12] L.W. Florschuetz, D.E. Metzger, C.C. Su, Heat transfer characteristics for jet array impingement with initial crossflow, J. Heat Transfer 106 (1984) 34–41.
[13] L.W. Florschuetz, Y. Isoda, Flow distributions and discharge coefficient effects for jet array impingement with initial crossflow, J. Eng. Power 105 (1983) 296–303.
[14] L.W. Floschuetz, C.C. Su, Effect of crossflow temperature on heat transfer within an array of impinging jets, J. Heat Transfer 109 (1987) 74–82.
[15] K.R. Saripalli, Visualization of multijet impingement flow, AIAA J. 21 (4) (1983) 483–484.
[16] A.I. Behbahani, R.J. Goldstein, Local heat transfer to staggered arrays of impinging circular air jets, J. Eng. Power 105 (1983) 354–360.
[17] S.J. Slayzak, R. Viskanta, F.P. Incropera, Effect of interaction between adjacent free surface planar jets on local heat transfer from

the impingement surface, Int. J. Heat Mass Transfer 37 (2) (1994) 269–282.
[18] S.A. Salamah, D.A. Kaminski, Modeling of turbulent heat transfer from an array of submerged jets impinging on a solid surface, Numer. Heat Transfer: Part A: Appl. 48 (4) (2005) 315–337.
[19] L.A. El-Gabry, D.A. Kaminski, Numerical investigation of jet impingement with cross flow - Comparison of Yang-Shih and standard k–ε turbulence models, Numer. Heat Transfer: Part A: Appl. 47 (5) (2005) 441–469.
[20] A.M. Huber, R. Viskanta, Effect of jet–jet spacing on convective heat transfer to confined, impinging arrays of axisymmetric air jets, Int. J. Heat Mass Transfer 37 (18) (1994) 2859–2869.
[21] J.Y. San, M.D. Lai, Optimum jet-to-jet spacing of heat transfer for staggered arrays of impinging air jets, Int. J. Heat Mass Transfer 44 (21) (2001) 3997–4007.
[22] B.P.E. Dano, J.A. Liburdy, K. Kanokjaruvijit, Flow characteristics and heat transfer performances of a semi-confined impinging array of jets: effect of nozzle geometry, Int. J. Heat Mass Transfer 48 (3–4) (2005) 691–701.
[23] R.J. Goldstein, J.F. Timmers, Visualization of heat transfer from arrays of impinging jets, Int. J. Heat Mass Transfer 25 (12) (1982) 1857–1868.
[24] W.M. Yan, H.C. Liu, C.Y. Soong, W.J. Yang, Experimental study of impinging heat transfer along rib-roughened walls by using transient liquid crystal technique, Int. J. Heat Mass Transfer 48 (12) (2005) 2420–2428.
[25] T. Wang, M. Lin, R.S. Bunker, Flow and heat transfer of confined impingement jets cooling using a 3-D transient liquid crystal scheme, Int. J. Heat Mass Transfer 48 (23–24) (2005) 4887–4903.